Comparative review of efficiency analysis for airborne solid submicrometer particle sampling by nuclepore filters

Maiqi Xiang, Martin Morgeneyer, Florian Philippe, Maheandar Manokaran, Christophe Bressot

Comparative Review of Efficiency Analysis for Airborne Solid Submicrometer Particle Sampling by Nuclepore Filters

Maiqi XIANG[1,2,*], Martin MORGENEYER[1], Florian PHILIPPE[1,2], Maheandar MANOKARAN[1], Christophe BRESSOT[2]

1. Génie de procédés Industriels, Sorbonne Universités, Université de Technologie de Compiègne (UTC), Compiègne, France
2. Direction des Risques Chroniques, Institut National de l'Environnement Industriel et des Risques (INERIS), Verneuil en Halatte, France

Abstract: Characterization and analysis of airborne solid submicrometer particles have received considerable attention. Representative collection of particles to be analyzed is a fundamental requirement. Herein we review the efficiency of particle sampling using Nuclepore filters. The available theoretical models based on different collection mechanisms: diffusion, interception, and impaction, are explored and compared. Experimentally measured values are combined to analyze the effect of the particle capturing mechanism on collection efficiency based on different parameters like filter pore size and flow face velocity. In addition, a method for experimental collection efficiency analysis combined with theoretical modeling is developed by considering the model's applicability. The diffusion model proposed by Marre fits the sampling conditions with a small most penetrating particle size (MPPS). The combined efficiency models have corrected the inappropriateness of considering particle deposition mechanisms separately. They are recommended if the assumptions are satisfied.

Keywords: collection efficiency models; particle capturing mechanisms; submicrometer particles; Nuclepore filter

1. Introduction

Submicrometer particles can have adverse health effects because of their direct effects or carrying toxic compositions (Elsaesser and Howard, 2012; Shatkin, 2017). Based on the same mass, submicrometer particles have large specific surface areas and easily interact with biological systems (Albanese et al., 2012). Once small particles are inhaled, they may not be removed from the human upper respiratory tract. They have high deposition rates in the alveolar region and, pass into the bloodstream (Salma et al., 2015). Finally, various diseases are produced, such as pulmonary inflammation, cardiovascular disease, heart disease, and respiratory tract damage (Mengersen et al., 2011; Schmid and Stoeger, 2016). Additionally, negative environmental effects of submicrometer particles have also been proven (Slezakova et al., 2013). Many studies have focused on cleaner production of nanoparticles and characterization of nanoparticle exposure, especially workplace exposure (Bressot et al., 2018; Fabiano et al., 2019; Morgeneyer et al., 2018; Todea et al., 2017). Particle analysis techniques, such as electron microscopy, have provided the possibility to determine both properties of the particle system (size and shape distributions) as well as those at the level of individual particles (structure and compositions) (Methner et al., 2012; Methner et al., 2010). Thus, the typical collection of particles to be analyzed is a prerequisite. Filtration, as a basis of characterization, has been used in various applications, such as air purification, respiratory protection, nuclear, and hazardous material processing (Chen et al., 2014; Easty et al., 2015; Huang and Yang, 2006). Filtration with Nuclepore filters is discussed herein because they are ideally suited for particle counting and image analysis (Romo-Kröger, 2006; Yamamoto et al., 2004). Nuclepore filters are developed by Price and Walker (1962), Fleischer et al. (1965) as well as their collaborators. They are porous analytical filters, commercially available for more than 10 years with 6 – 12 µm thickness and 13 – 47 mm diameter. Pores are distributed on the filter surface with a uniform size (Heidam, 1981). There are various

pore sizes available, mostly ≤ 12 μm with a porosity ≤ 20%. Nuclepore filters are suitable for microfiltration, and for direct observation of cells, viruses, organelles, particles, diesel soot, and fibers by both light and electron microscopy (Chen et al., 2014; Chen et al., 2013b). Godoi et al. (2016) collected particulate matter resuspended in two rural ultramafic rock roads using Nuclepore filters with 47 mm diameter and 0.4 μm pore size. Representative aerosol compositions for the resuspended particulate matter at regional scales were assessed. Results showed that inhalable suspended chrysotile near local roads was related to the frequent development of lung cancer in the population of long-term exposed regions. Lafleur et al. (2015) deposited *S. aureus* N315 onto Nuclepore filter with 25 mm diameter and 0.2 μm pore size, which made subsequent assessment easy with image analysis software. Nuclepore filters have sampling efficiencies as high as 99% (Cyrs et al., 2010) for capturing submicrometer particles (Chen et al., 2013a).

To get high sampling efficiencies, the theoretical collection mechanisms of Nuclepore filters are worth to be explored. Since the structure of Nuclepore filters is like a group of parallel circular capillaries, the capillary tube models developed in the 1960-1970s can be used to calculate the collection efficiency. In the capillary tube model, the number of pores per surface unit of the filter is expressed as N_0. The pore radius is r_0 and the pore area is A_0. The ratio of pore area to total filter area is porosity P: $P = A_0N_0 = \pi {r_0}^2 N_0$ (Manton, 1978, 1979). The filter thickness is L_f. The aerodynamics of a unitary pore can be modeled by Fig. 1. When air with a radius r_c passes through a unitary pore, particles are collected by filter surface, or filter pore wall, here $r_\mathrm{c} = r_0/\sqrt{P}$ (Manton, 1978, 1979). Three distinct capture mechanisms were found: a) capture of small particles by diffusion, b) capture of large particles by impaction, and c) interception (Rubow, 1981; Spurny et al., 1969), as shown in Fig. 2 (Bulejko, 2018). The overall collection efficiency is calculated according to these deposition mechanisms, which can be expressed as (Hinds, 1999):

$$E = 1 - (1 - E_\mathrm{DW})(1 - E_\mathrm{DS})(1 - E_\mathrm{R})(1 - E_\mathrm{I}) \quad (1.)$$

Where, E_DW, E_DS, E_R, E_I are sampling efficiencies due to diffusion deposition on the pore wall, diffusion deposition on the filter surface, interception deposition on the pore wall and impaction deposition on the filter surface respectively. In general, they are functions of particle diameter.

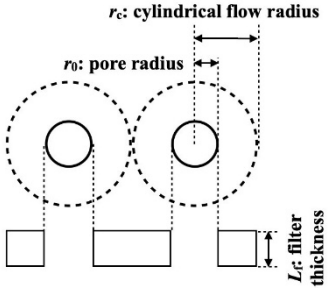

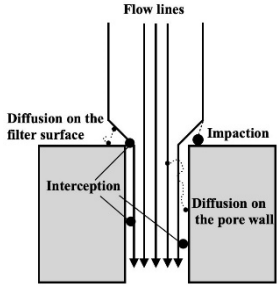

Fig. 1. Characterization of unitary pore

Fig. 2. Capture mechanisms involved in one capillary pore of Nuclepore filters

Many models have been proposed for calculating the primary particle sampling efficiency due to individual mechanisms. Spherical particles are generally assumed (Gentry et al., 1982). However, such models should be carefully selected according to their applicability. The current review explores and compares the available theoretical models to assess the sampling efficiencies of Nuclepore filters. Particle deposition mechanisms including diffusion, interception, and impaction are involved. The overall sampling efficiency and the surface sampling efficiency are investigated for different sampling situations to analyze the effect of the particle capturing mechanisms. In addition, a method for experimental efficiency analysis when combining theoretical models is proposed based on the model's applicability.

2. Theoretical Models for Efficiency Analysis

In the beginning, the filtration theories were explained by Fleischer et al. (1965) and Price and Walker (1962). Then Spurny summarized a series of theoretical models (Hampl and Spurný, 1966; Spumy and Pich, 1965; Spurný and Pich, 1963, 1965; Spurny and Pich, 1964) and developed the most classic one (Spurny et al., 1969). Smith et al. (1976) pointed out that besides diffusing on the wall of filter pores, particles can also diffuse onto the surface of filters, which has been proved to be of great significance. Marre et al. (2001) took into account the effects of flow slip on the sampling efficiency in the intermediate crossover regime between Brownian diffusion and interception. Here the models of sampling efficiency referring to individual capture mechanisms are explored respectively. Each model is calculated by formulae using MATLAB. In the gas flow field, air with a face velocity of U_0 passes through the unitary pore. U_0 is the speed at which the carrier fluid approaches the filter membrane. The Reynolds number *Re*, defined as:

$$R_e = r_c U_0 / \upsilon \tag{2.}$$

Where υ is the kinematic fluid viscosity. U_0 is given by the flowrate Q and the section area of the filter:

$$U_0 = Q/(\pi/4){d_f}^2 \tag{3.}$$

d_f is the filter diameter.

Diffusion Efficiency

Brownian diffusion is a significant mechanism for capturing small particles, which has been described by a linear transport equation proposed by Fuchs (1965). Diffusion efficiency E_D is determined by the diffusion coefficient (Mercer and Greene, 1974; Park et al., 1980). The early researches only paid attention to the diffusion efficiency due to pore wall deposition. Smith et al. (1976) and Manton (1979) found that particles could also deposit on the front surface of Nuclepore filters with a non-negligible amount. Subsequently, Gentry et al. (1982); Rubow and Liu (1986) and Cyrs et al. (2010) confirmed this with experimental data.

Diffusion Efficiency due to Pore Wall Deposition

The sampling efficiency due to diffusion on the wall of filter pores was computed by Gormley and Kennedy (1948), Twomey (1962) and Spurny et al. (1969), which related to diffusion parameter N_D:

$$N_D = \frac{L_f D P}{r_0^2 U_0} \tag{4.}$$

Where D is the particle diffusion coefficient varying with particle size (Park et al., 1980), which can be calculated by Stokes-Einstein Equation (Hinds, 2012; Li et al., 2002).

In the range of $N_D < 0.01$, Gormley and Kennedy (1948) calculated the diffusion efficiency due to pore wall deposition E_{DW} as:

$$E_{DW} = 2.56{N_D}^{2/3} - 1.2N_D - 0.177{N_D}^{4/3} \tag{5.}$$

For $N_D > 0.01$, the equation of Twomey (1962) was mostly used:

$$E_{DW} = 1 - 0.81904\exp(-3.6568N_D) - 0.09752\exp(-22.3045N_D) - 0.03248\exp(-56.95N_D) - 0.0157\exp(-107.6N_D) \tag{6.}$$

Subsequently, Gentry et al. (1982) applied models proposed by Park et al. (1980) into Nuclepore filters and got another expression of E_{DW}:

$$E_{DW} = 1 - 0.819exp(-3.65P_e^{-1}) - 0.097exp(-22.3P_e^{-1}) - 0.035exp(-57P_e^{-1}) \tag{7.}$$

For $Pe \leqslant 25$ and

$$E_{DW} = 2.56P_e^{-2/3} - 1.2P_e^{-1} - 0.177P_e^{-4/3} \tag{8.}$$

For $Pe > 25$.

Where the Peclet's number *Pe* was given by

$$Pe = \frac{U_0}{\pi D N_0 L_f} = \frac{1}{N_D} \tag{9.}$$

In 2001, Marre et al. (2001) predicted that flow slip at the pore wall of filters might affect the particle capturing, especially might enhance the sampling efficiency in the intermediate crossover regime between Brownian diffusion and direct interception. Considering the flow slip, E_{DW} in the crossover regime was calculated by:

$$E_{\mathrm{DW}} = \frac{4{y_d^*}^2}{1+4N_G}\left(1+2\frac{N_G}{y_d^*}\right) \tag{10.}$$

$$N_G = N_g\left(1+N_g/2\right) \tag{11.}$$

$$N_g = l_g/r_0 \tag{12.}$$

Where *lg* is the slip length (Marre et al., 2004). y_d^*, normalized distance, is a parameter related to N_G and γ. γ is a parameter related to D, given by:

$$\gamma = \frac{U_0{r_0}^2}{DL_{\mathrm{f}}} \tag{13.}$$

For viscous fluids, when neglecting flow slip, E_{DW} in the crossover regime was calculated as:

$$E_{\mathrm{DW}} = \frac{2^{4/3}\gamma^{-2/3}}{1+4N_G}\left(1+2^{4/3}N_G\gamma^{1/3}\right) \tag{14.}$$

Fig.3 shows theoretical models for calculating diffusion efficiency due to pore wall deposition simulated by Spurny, Gentry, and Marre respectively. Similar curve trends are displayed. Calculations of Spurny and Gentry have the same curve. Both of these models use the Gormley-Kennedy Equation. Model of Marre shows higher efficiencies than those of Spurny and Gentry for submicrometer particles.

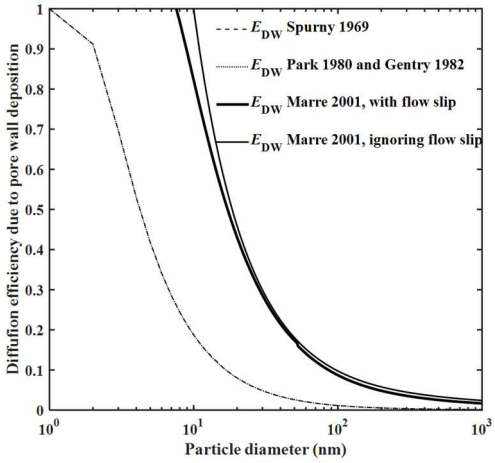

Fig. 3. Theoretical models of diffusion efficiency due to pore wall deposition (models of Spurny and Gentry overlap) (r_0 = 1 μm, P = 0.1, L_f = 9 μm, U_0 = 2 m/s, ρ_p = 2000 kg/m^3)

Diffusion Efficiency due to Surface Deposition

With the progressive researches of diffusion efficiency, numerous reports (Chen et al., 2013a; Park et al., 1980; Smith et al., 1976) proposed that surface deposition is also a dominant mechanism for collecting particles smaller than 100 nm.

Manton (1979) elicited model of diffusion efficiency due to surface deposition E_{DS}:

$$E_{\mathrm{DS}} = 1 - exp\left\{-\frac{\alpha_1 \mathcal{D}^{2/3}}{\left[1+(\alpha_1/\alpha_2)\mathcal{D}^{7/15}\right]}\right\} \tag{15.}$$

Where α_2 = 4.5, $\mathcal{D} = D/r_{\mathrm{c}}U_0$ is the normalized diffusion coefficient, α_1 is a parameter determined by the least-squares fitting, which related to the filter porosity. This model has been used in many recent researches. Its applicability has been verified in the porosity range of 0.05-0.64 (Chen et al., 2013a; Cyrs et al., 2010; Ogura et al., 2016).

Gentry et al. (1982) also pointed out that the values calculated by Eqs. (7-9) underestimated the diffusion efficiency.

Assumed that the densities of particles deposited on the surface and deposited on the pore wall of filters are the same, the diffusion efficiency can be expressed as:

$$E_{\mathrm{D}}(corrected) = E_{\mathrm{DW}} A_R \tag{16.}$$

Where A_R is the total exposed surface area (the total area of filter pore wall and filter face). Then E_{DS} can be calculated as:

$$E_{\mathrm{DS}} = 1 - \frac{1 - E_{\mathrm{DW}} A_R}{1 - E_{\mathrm{DW}}} \tag{17.}$$

The models for calculating diffusion efficiency due to surface deposition are compared in Fig. 4. Mostly, Gentry's model shows higher efficiency, especially for small particles (Fig. 4(a)). When pore size is small or porosity is high, the model of Manton shows slightly higher efficiency for large particles (Fig. 4(b)). However, owing to the approximate estimation, the model proposed by Gentry is not a priority.

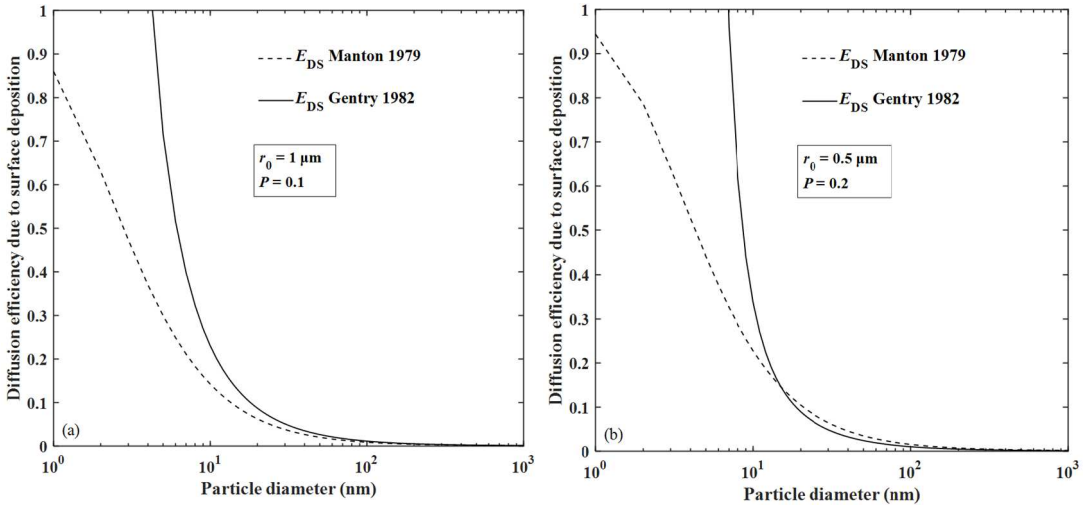

Fig. 4. Theoretical models of diffusion efficiency due to surface deposition (L_f = 9 μm, U_0 = 2 m/s, ρ_p = 2000 kg/m^3; and (a) r_0 = 1 μm, P = 0.1; (b) r_0 = 0.5 μm, P = 0.2)

Interception Efficiency

If a particle touches the filter when it is moving by, interception occurs. Interception efficiency depends on particle size and pore size.

For uniform flow, the most famous theoretical model is the one proposed by Spurny et al. (Spurny et al., 1969), which is also the same as that put forward by Natanson (1957):

$$E_{\mathrm{R}} = N_r(2 - N_r) \tag{18.}$$

where $N_r = r_{\mathrm{P}}/r_0$. r_{P} is the particle radius.

This expression assumes that particles have finite sizes and the inertia of particles related to the flow is neglected. When a particle approaches the pore entrance from a distance, the streamline curves incline towards the axis. When it is near the pore, the streamline curves incline towards the opposite direction. This drift across streamlines is caused by the particle's inertia.

Later, Smith et al. (1976) compared the particle capturing efficiency at the pore entrance between rectangular flow profile and laminar flow profile. For the rectangular profile, the interception efficiency equation is the same as Spurny's model. For the laminar profile, the efficiencies are lower since the flow near the pore wall is comparatively small. It can be expressed as:

$$E_{\mathrm{R}} = [N_r(2 - N_r)]^2 \tag{19.}$$

John and Reischl (1978) measured the collection efficiencies of 8 μm filters. Interception is a dominant filtration mechanism in this condition. For non-uniform flow (the stokes flow is determined due to the oblate spheroidal

coordinates), interception efficiency calculated by Happel and Brenner (2012) better fits his experimental results:

$$E_{\mathrm{R}} = [N_r(2 - N_r)]^{3/2} \quad (20.)$$

Gentry et al. (1982) agreed with the above models for interception efficiency calculation. However, in order to fit his experimental data of filtering nebulized small particles, another expression was more appropriate for Poiseuille flow:

$$E_{\mathrm{R}} = [N_r(2 - N_r)]^{2/3} \quad (21.)$$

The author stated that interception efficiency depends on the value of N_r. For example, the value of N_r in his test was 0.02 while in John's test (John and Reischl, 1978) was 0.4.

Marre et al. (2001) considered the effects of flow slip on interception efficiency for Poiseuille flow. The interception efficiency was described as:

$$E_{\mathrm{R}} = \frac{4N_R^2}{1 + 4N_G}\left(1 + 2\frac{N_G}{N_R}\right) \quad (22.)$$

$$N_R = N_r\left(1 - \frac{N_r}{2}\right) \quad (23.)$$

If the flow slip is ignored, the interception efficiency is calculated as in the model of Smith. Because of high convective flux of particles near the pore wall, flow slip brings higher efficiency.

In general, Equation $E_{\mathrm{R}} = [N_r(2 - N_r)]^a$ is suitable for interception efficiency calculation. It is valid when the particle size smaller than the pore size. Fig. 5 shows models developed by Spurny, Smith, John, Gentry, and Marre respectively. For uniform flow, "a=1" is consistent with the experimental results (Chen et al., 2013a). For non-uniform flow, "a=1" overestimates the interception efficiency and different values of "a" were proposed. Consequently, interception efficiency depends on the value of N_r. Flow type is also a crucial factor. When neglecting flow slip at the pore wall, "a=2" is recommended by Marre for Poiseuille flow. If the flow slip is considered, higher efficiencies are manifested than ignoring the flow slip, which depends on the filter pore size. It is notable that for the model with the value of "a=2/3" proposed by Gentry, the highest efficiency is shown, which is doubtful. Interception efficiency varies with flow type and parameter N_r (Gentry et al., 1982). More specific investigations are suggested to determine the effect of flow types and the value of N_r on interception efficiency.

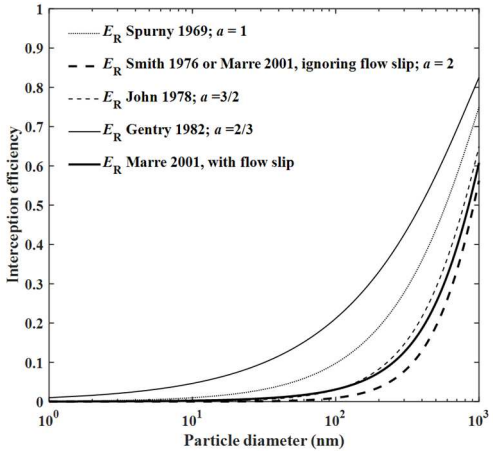

Fig. 5. Theoretical models of interception efficiency (r_0 = 1 μm, P = 0.1, L_f = 9 μm, U_0 = 2 m/s, ρ_p = 2000 kg/m^3)

Impaction Efficiency

If particles are too large to adequately respond to the change of flow direction, inertial impaction will occur.

In 1964, Pich (1964) put forward a classical theoretical model to estimate the impaction efficiency for aerosol particles passing through circular pores of a membrane ultrafilter. Laminar flow with parabolic streamlines and constant flow velocity in the flow direction are supposed in this model. The impaction efficiency is calculated as:

$$E_{\mathrm{I}} = \frac{2\varepsilon_i}{1+\xi} - \left(\frac{\varepsilon_i}{1+\xi}\right)^2 \tag{24.}$$

$$\varepsilon_i = 2Stk\sqrt{\xi} + 2Stk^2\xi exp\left[-\frac{1}{Stk\sqrt{\xi}}\right] - 2Stk^2\xi \tag{25.}$$

$$\xi = \frac{\sqrt{P}}{1-\sqrt{P}} \tag{26.}$$

Stk is the Stokes number.

This model is described in Fig. 6. The impaction efficiency increases with particle size.

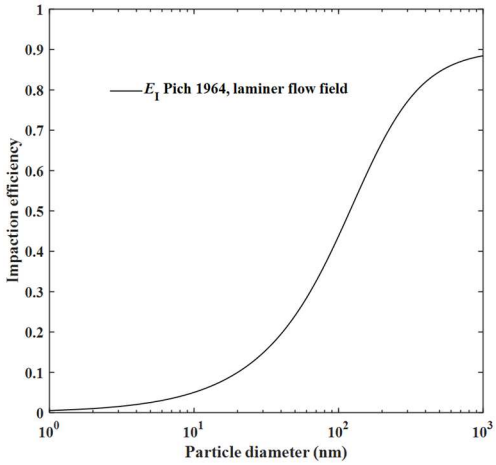

Fig. 6. Theoretical models of impaction efficiency (r_0 = 1 μm, P = 0.1, L_f = 9 μm, U_0 = 2 m/s, ρ_p = 2000 kg/m^3)

Combined Efficiency of Impaction and Interception

Interception efficiency calculated by most developed models omits the particle inertia relative to the flow, while Pich's impaction efficiency model neglects the finite size of particles. It is inappropriate to consider impaction and interception separately. Manton (1978) expounded on the combined efficiency of impaction and interception. Parabolic flow is supposed in this model. The collection efficiency due to the combined mechanisms of impaction and interception E_{IR} was calculated as:

$$E_{\mathrm{IR}} = \{N_r(2-N_r)\}^{\frac{2}{1+aN_r+bN_r^2}} \tag{27.}$$

a and *b* are functions of inertia parameter *I*.

$$I = \frac{2\rho_{\mathrm{p}}ReP}{9\rho} \tag{28.}$$

Where ρ is the flow density. The filter porosity assumed in this model is between 0.04 and 0.36. This model has been verified when the Stokes number is less than 100 and "*I*" value is greater than 1.35 (Chen et al., 2013a).

The overall collection efficiency is calculated as:

$$E = 1-(1-E_{\mathrm{IR}})(1-E_{\mathrm{DW}})(1-E_{\mathrm{DS}}) \tag{29.}$$

Combined Efficiency of Diffusion and Interception

Marre et al. (2001) indicated that there was higher efficiency in the intermediate crossover regime between diffusion and direct interception for Nuclepore filters. Considering the flow slip, the filtration efficiency in the intermediate crossover regime between diffusion and interception E_{DR} was given by

$$E_{\mathrm{DR}} = \frac{4y^{*2}}{1+4N_G}\left(1+2\frac{N_G}{y^*}\right) \tag{30.}$$

Where y^* is a parameter related to N_R, N_G, and γ.

If the flow slip is neglected, the collecting efficiency of cylindrical pore reduces, which can be described by the limiting expressions of Brownian diffusion for small particles and interception for large particles:

$$E_{\mathrm{DR}} \to \begin{cases} equation\ (12) & for\ r_{\mathrm{p}} \ll \mathrm{MPPS} \\ equation\ (17) & for\ r_{\mathrm{p}} \gg \mathrm{MPPS} \end{cases} \quad (31.)$$

Here MPPS is the most penetrating particle size, in which all the filtration capture mechanisms have little effect and the total collection efficiency is lowest. The corresponding efficiency is the minimum efficiency (ME).

The overall collection efficiency is calculated as:

$$E = 1 - (1 - E_{\mathrm{DR}})(1 - E_{\mathrm{DS}})(1 - E_{\mathrm{I}}) \quad (32.)$$

3. Experimental Efficiency Analysis

Various types of Nuclepore filters are commercially available. A multitude of experimental work combining the theoretical models has been carried out to determine the filter collection efficiencies as well as the related influence factors (John and Reischl, 1978; Liu et al., 1976; Montassier et al., 1996). In general, the particles generated by an atomizer are captured by a Nuclepore filter then counted by an aerosol detector. For working with a globally neutral aerosol, a neutralizer is generally placed upstream of the filter. Mobility equivalent diameter is chosen mostly because electrical aerosol detection equipment, e.g., scanning mobility particle sizer (SMPS) is usually used for submicrometer particle measurement in recent years. Gentry et al. (1982) reported that the overall collection efficiencies of 2 μm filter for 42 nm NaCl particles were 55%–65% at flowrates in the range of 0.73–1.3 L/min. Burton et al. (2006) found that for 1 and 3 μm Nuclepore filters with a flowrate of 4 L/min, the lowest overall collection efficiencies were 49% and 22% respectively. In some investigations, e.g. (Zíková et al., 2015), low overall collection efficiencies, i.e. even as low as 3% were observed for Nuclepore filters. In addition, when using electron microscopy, particles collected on the filter surface can be determined, which refers to the surface collection efficiency (E_S). This part expounds experimental overall collection efficiency and surface collection efficiency of Nuclepore filters. Different models are selected for fitting these tests. Influence factors are combined to explore the impacts of the capturing mechanisms on sampling efficiency. Particle type and size, filter properties, as well as flow conditions involved in the tests are summarized in Table 1.

Reference	Particle type	Particle size, nm	Pore size, μm	Porosity, %	Filter thickness, μm	Face velocity, cm/s
Spurny et al. (1969)	Pt, Se, NaCl	2-500	0.5, 0.8, 1, 2, 5, 8	5.1, 2.5, 3.9, 6.3, 7.8, 5	12, 11, 10, 8, 8, 10	1-10
Liu et al. (1976)	DOP	30-1000	0.6, 1, 3, 5, 8	8.4, 15.6, 14.1, 7.8, 5	10	5-500
Gentry et al. (1982)	NH4-fluorescein	>40	1, 3, 5, 8	—	—	0.8-6.6
	NaCl	>40	2, 3, 5			0.8-6.6
	NaCl	8-24	2, 3, 5, 8, 12			0.8-6.6
	Ag	8-24	5, 8			1.5-8
Cyrs et al. (2010)	KCl	9-402	0.4, 0.8	6.4, 7.3	10.6, 10.5	3.7, 18.4
Chen et al. (2013a)	PSL, Ag, NaCl	20-800	1, 3	16, 14	11, 9	2-15
Soo et al. (2016)	NaCl	10–400	0.4, 0.8, 2, 5	—	—	3.08-20.5
Ogura et al. (2016)	Ag/	15-30/	0.08	1.9	6	1.9, 8.4
	PSL	30-800	0.2	6.3	10	1.5, 8.6

Table 1 Particle properties, filter properties and flow conditions involved in the tests

Overall Collection Efficiency

Spurny et al. (1969) measured the collection efficiencies of Nuclepore filters for different particle types to verify his theoretical model. Geiger-Muller tubes and a dual-channel impulse counter were used to measure the collection

efficiency. His results showed that when a 5 μm filter was used to collect Selenium aerosol at a face velocity of 5 cm/s, the minimum efficiency was about 5%, corresponding to an MPPS of about 90 nm. In the theoretical overall efficiency calculations, the diffusion efficiency due to surface deposition was not included. After expanding Eq. (1), and ignoring the small terms of $E_{DW}E_R$ and $E_{DW}E_IE_R$, the theoretical models still overestimated the overall sampling efficiency. Therefore, a weighting factor 0.15 was included in the term of E_R empirically. The theoretical model became

$$E = E_{DW} + E_I + 0.15E_R - E_IE_D - 0.15E_IE_R \quad (33.)$$

However, this calculation ignores the term $E_{DW}E_IE_R$ - $E_{DW}E_R$, which may offset the overestimation of the overall collection efficiency.

Liu et al. (1976) investigated the collection efficiencies of several common Nuclepore filters for collecting monodisperse DOP particles at different face velocities using an electrical aerosol detector. Results reported that the particle capturing mechanisms of interception, impaction, and diffusion are significant. For small pore size filters (0.6 and 1 μm) in the condition of small pressure drop (less than 13 kPa), the MPPS decreased with pressure drop. For large pore size (3, 5, 8 μm) filters or high pressure drop (13-40 kPa) conditions, the sampling efficiency increased with particle size (30-1000 nm) and pressure drop. This means the prominent particle collecting mechanisms for large pore size filters or high-pressure drop sampling are impaction and interception, which is consistent with the particle behavior predicted by theoretical models.

Gentry et al. (1982) surveyed the fractional penetrations of the diffusion battery Nuclepore filter section for different types of particles. The fractional penetration was obtained by the ratio of downstream and upstream concentrations using a condensation nuclei counter. In the theoretical efficiency calculations, the impaction efficiency was ignored:

$$E = 1 - (1 - E_D)(1 - E_R) \quad (34.)$$

Results showed that for particles diameter smaller than 30 nm, particles uniformly distributed on the filter face, while for particles diameter larger than 40 nm, particles preferred to concentrate near the rims of the pores. For Ag particles with a size of 8-24 nm, E_{DS} was paramount especially when the face velocity was less than 10 cm/s. For particles larger than 40 nm, the theoretical expressions used here underestimated the particle collection efficiencies, because the impaction efficiency was ignored.

Surface Collection Efficiency

Cyrs et al. (2010) collected submicrometer particles using capillary pore membrane filters and measured the surface collection efficiencies by scanning electron microscope (SEM) and overall collection efficiencies by SMPS. The surface collection efficiency here was calculated as:

$$E_S = 1 - (1 - E_{DS})(1 - E_I) \quad (35.)$$

Results showed that the theoretical model fits experimental overall collection efficiency very well but had a discrepancy with surface collection efficiency when particle size larger than 100 nm. Especially for 0.8 μm filter with a surface velocity of 18.4 cm/s, the experimental efficiency for collecting 237 nm particles was about 58% higher than the theoretical value. The possible reason is that for big particles, interception is a prominent deposition mechanism. When counting particles using the electron microscope, particles deposed due to interception may be falsely counted. The overall collection efficiencies were much higher than surface efficiencies especially for small pore size filters, but had the same trends. This means particle deposition on the wall of filter pores cannot be neglected. The small pore size filters have greater surface areas of pore wall.

In the research of Chen et al. (2013a), the number distribution of submicrometer particles collected on the filter surface was calculated by the method of Cyrs et al. (2010), but the interception efficiency was also included. The theoretical model for calculating surface collection efficiency became

$$E_S = 1 - (1 - E_{DS})(1 - E_R)(1 - E_I) \quad (36.)$$

The overall collection efficiencies and surface collection efficiency were compared by theoretical models and experiments using SMPS and SEM. Different particle sizes and densities, filter pore sizes, and flow face velocities were considered. Two particle sampling models were compared to fit the experimental overall collection efficiency. The first one was a modification based on the theory of Spurny et al. (1969) (Eqs. (4-6), (15), (18), and (24-26)). The other was the model of Manton (Manton, 1978, 1979) (Eqs. (4-6), (15) and, (27-28)), which considered the combined efficiency of impaction and interception. Results showed that the calculation of Manton yielded results closer to experimental overall collection efficiency than the model of Spurny for "I" value between 1.35 and 7.6. When the value of "I" was less than 0.85, it was not appropriate anymore and the modified Spurny model was better. In this situation, the difference between values calculated by the modified Spurny model and experimental surface collection efficiency was less than 10.3%.

In addition, Ogura et al. (2016) measured the surface collection efficiencies of small pore size Nuclepore filters by SEM and a condensation particle counter. Besides Eq. (36), the following theoretical equation was compared to fit the experimental surface efficiency:

$$E_S = 1 - (1 - E_{DS})(1 - E_{IR}) \quad (37.)$$

Results showed that the measured surface collection efficiencies of 0.08 and 0.2 μm filters were greater than 60% at face velocities of 1.5 - 8.6 cm/s, which were not consistent with the theoretical values very well. The possible reason is that the sampling conditions exceed the model's applicability. For example, the value of "I" and P are too low to use the models of Manton (Manton, 1978, 1979). In addition, the usability of theoretical models for super small pore size filters (<0.4 μm) still needs to be verified.

The models used in the experimental work have been listed in Table 2. In general, for the overall collection efficiency, experimental data are consistent with theoretical efficiencies. However, for the surface collection efficiency, the results don't fit very well. On the one hand, considering the applicability of each model is very important; on the other hand, the counting method for electron microscopy observation should be uniform, and the contribution of interception deposition on surface efficiency should be defined.

Collection efficiency \ Authors	Spurny et al. (1969)	Gentry et al. (1982)	Cyrs et al. (2010)	Chen et al. (2013a)	Ogura et al. (2016)
E_{DW}	Eqs. (4-6)	Eqs. (7-9)	Eqs. (4-6)	Eqs. (4-6)	—
E_{DS}	—	Eq. (17)	Eq. (15)	Eq. (15)	Eq. (15)
E_R	Eq. (18)	Eq. (21)	Eqs. (22-23)	Eq. (18)	Eqs. (22-23)
E_I	Eqs. (24-26)	—	Eqs. (24-26)	Eqs. (24-26)	Eqs. (24-26)
E_{IR}	—	—	—	Eqs. (27-28)	Eqs. (27-28)
E	Eq. (33)	Eq. (34)	Eq. (1)	Eq. (1) or (29)	—
E_S	—	—	Eq. (35)	Eq. (36)	Eq. (36) or (37)
Fit or not	yes	yes	yes for E	yes	not very well

Table 2 Theoretical models used in the tests

Influence Factors

For most Nuclepore filters, the collection efficiency curve shows a U-shape with a minimum (Chen et al., 2013a; Montassier et al., 1996; Soo et al., 2016; Spurny, 1998). The efficiency strongly depends on filter properties and filtration conditions such as filter type, pore size, porosity, particle size, and airflow velocity according to the theoretical models. Similar results have been observed in various tests (Caroff et al., 1973; Liu et al., 1983; Montassier et al., 1996; Zíková et al., 2015).

Effect of Pore Size and Time

Small filter pore sizes are required for capturing nanoparticles. When the pore size is less than the particle size, the collection efficiency is approximately 1. The overall collection efficiency decreases with pore size. However, the effect of pore size on surface collection efficiency is unclear, as shown in Fig. 7. In addition, the effective pore size and pore numbers decrease by the accumulation of particles around the pore edge, which increases the collection efficiency (Fan et al., 1978a; Fan et al., 1978b; Soo et al., 2016; Spurny et al., 1969). Yamamoto et al. (2004) detected that the collection efficiency increased by 2% for 2 μm filter at 0.48 cm/s face velocity when sampling 200 nm PSL particles for 100 minutes.

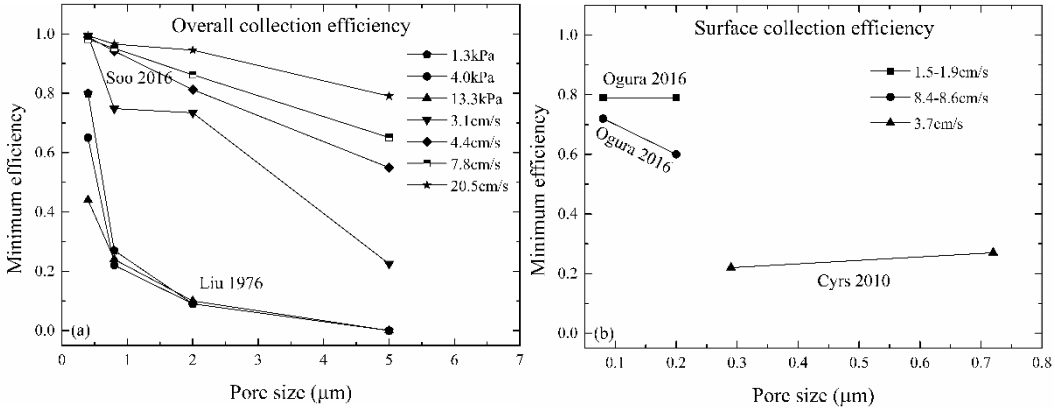

Fig. 7. Effect of pore size on collection efficiency

Effect of Flow Face Velocity

For most Nuclepore filters, the MPPS becomes smaller as the face velocity increases. Increasing face velocity causes an increased probability of particle deposition due to inertial impaction and interception, which will increase the collection efficiency for big particles (Gentry et al., 1982), as shown in Fig. 8. The experimental data of Smith et al. (1976) also indicated that the increase of face velocity led to a sharper cut-off, which could regulate the 50% cut-point size.

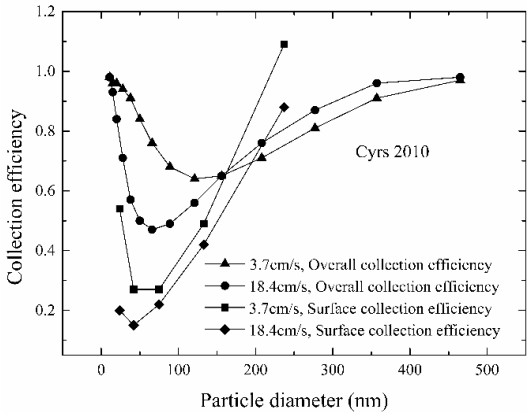

Fig. 8. Effect of face velocity on collection efficiency

Effect of Particle Size and Particle Density

For different particle sizes, the main mechanisms for collecting particles are different. Small particles are easily collected by diffusion mechanism; while big particles tend to be collected by impaction or interception. For particle size larger than filter pore size, a 100% overall and surface collection efficiency were observed in the experiments (Liu et al., 1976; Ogura et al., 2016). In addition, according to Ogura et al. (2016), the difference in surface collection efficiency using Nuclepore filters between the collection of PSL and Ag particles was up to 20%. According to the theoretical models, particle density affects the value of *Stk*, thereby affecting the impaction efficiency.

Effect of Particle Shape

Particle shape has effects on sampling efficiency. For primary sphere-like particles, this effect is negligible. For non-spherical particles, e.g., agglomerates, and nanomaterials, particle characteristics should be explored to discuss particle deposition mechanisms. The dynamic shape factor and the maximum length of agglomerates can be added to the theoretical calculations to describe the effect of particle shape on interception deposition and impaction deposition (Chen et al., 2013b). Gentry and Spurny (1978) discussed the collection efficiency of asbestos fibers and found that the pore size of filters and the face velocity were still the main factors. Gao et al., (2020) deliberated on the equivalent diameter of graphene nanoplatelets (GNPs) with plate-like shapes and folded structures. Results showed that the plate-like GNPs had higher capture efficiency than sphere-like NaCl particles due to the larger interception length. Jeffery (1922) and Cheng et al. (1991) pointed out that the orientation distribution of elongated particles affects the collection efficiency.

4. Efficiency Analysis Method Combined with Models

It's a good way to discuss the experimental collection efficiency by investigating the particle deposition mechanisms. A synthetical method is proposed to choose appropriate models for fitting the experimental data. A selection guide of available theoretical models to assess the sampling efficiency of the Nuclepore filter is presented in Table 3. For individual particle capturing mechanism, the controversial models are removed after the comparison between the models. Three models for diffusion efficiency due to pore wall deposition, one model for diffusion efficiency due to surface deposition, four models for interception efficiency, and one model for impaction efficiency are listed. For the overall collection efficiency calculation, besides the universally model (Eq. (1)) (Eqs. (33) and (34) have been corrected to Eq. (1) empirically), models referring to the combined efficiency of impaction and interception (Eq. (29)), and the combined efficiency of wall diffusion and interception (Eq. (32)) are included. In addition, according to the sampling and observation conditions, three models for calculating the surface collection efficiency are investigated. Using this method, models for calculating sampling efficiency can be easily and accurately picked when fitting the experimental values. Two examples are listed to verify this method.

Theoretical efficiency	Conditions	Models	References
E_{DW}	Universally	Eqs. (4-6)	Spurny et al. (1969)
	Poiseuille flow; with flow slip; in the intermediate crossover regime between Brownian diffusion and direct interception	Eqs. (10-13)	Marre et al. (2001); Mathis et al. (2004)
	Poiseuille flow; flow slip neglected; in the intermediate crossover regime between Brownian diffusion and direct interception	Eq. (14)	Marre et al. (2001); Mathis et al. (2004)
E_{DS}	P = 0.05-0.2	Eq. (15)	Manton (1979)
E_R	Uniform flow or Rectangular flow profile	Eq. (18)	Smith et al. (1976); Spurny et al. (1969)
	Poiseuille flow	Eq. (19)	Smith et al. (1976)
	Stokes flow	Eq. (20)	John and Reischl (1978)
	Poiseuille flow; flow slip neglected	Eq. (19)	Marre et al. (2001); Mathis et al. (2004)
	Poiseuille flow; with flow slip	Eqs. (22-23)	Marre et al. (2001); Mathis et al. (2004)
E_I	Laminar flow; constant flow velocity	Eqs. (24-26)	Pich (1964)
E_{IR}	Non-slip Poiseuille flow; P = 0.04-0.2; Stk < 100; I >1.35	Eqs. (27-28)	Chen et al. (2013a); Manton (1978)
E_{DR}	Poiseuille flow; with flow slip; in the intermediate crossover regime between Brownian diffusion and direct interception	Eq. (30)	Marre et al. (2001); Mathis et al. (2004)
E	—	Eq. (1)	Chen et al. (2013a); Cyrs et al. (2010)

	— (Inadequateness of considering E_I and E_R separately is corrected)	Eq. (29)	Chen et al. (2013a); Manton (1978)
	— (Inadequateness of considering E_{DW} and E_R separately is corrected)	Eq. (32)	Marre et al. (2001)
E_S	— (Interception deposition isn't included)	Eq. (35)	Cyrs et al. (2010)
	— (Interception deposition is included)	Eq. (36)	Ogura et al. (2016)
	— (Interception deposition is included)	Eq. (37)	Chen et al. (2013a); Ogura et al. (2016)

Table 3 Selection guide of theoretical efficiency models for Nuclepore filter sampling (spherical particle is assumed)

Case of Cyrs et al. (2010)

The work of Cyrs et al. (2010) has been summarized above. Here the case of calculating overall collection efficiency with a flow velocity of 3.7 cm/s and a pore size of 0.72 μm is analyzed. The Reynold number is 0.0033. The MPPS is big due to the low flow velocity and small Reynold number. The model of diffusion efficiency due to pore wall deposition proposed by Marre only fits in the case of the intermediate crossover regime between Brownian diffusion and direct interception, that is, it fits for a small range that includes the MPPS. It is not eligible for particle size much smaller than MPPS. Similarly, his model for calculating the combined efficiency of diffusion and interception is also not appropriate. Hence, Eqs. (10-13), (14), and (32) are not suitable in this case. In addition, the inertia parameter "*I*" in this test is 0.1267, which is too small to use the model of Manton (Eqs. (27-28)).

In conclusion, the model of Spurny (Eqs. (4-6)) for calculating the diffusion efficiency due to pore wall deposition; the model of Manton (Eq. (15)) for calculating the diffusion efficiency due to surface deposition; and the model of Pich (Eqs. (24-26)) for calculating the impaction efficiency are picked. For the interception efficiency calculation, Eqs. (18) and (20) are compared, as shown in Fig. 9 (a) and (b). The overall collection efficiency calculated by models of Marre (Eqs. (10-13) for E_{DW} and (22-23) for E_R) is added for comparison, as shown in Fig. 9 (c).

Results show a good theory-experiment convergence when Eq. (18) is used to calculate the overall collection efficiency. The theoretical MPPS is around 140 nm, corresponding to a minimum efficiency, about 63.5%. Theoretical efficiency calculated by models of Marre shows a big difference with the experimental values, which verifies the inappropriateness of Marre's model for calculating diffusion efficiency when MPPS is big.

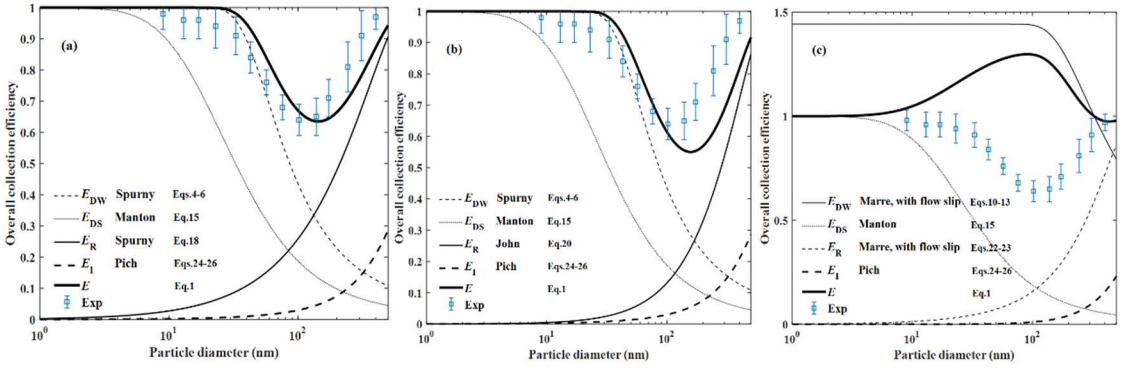

Fig. 9. Comparison of experimental and theoretical approaches for assessing overall collection efficiency using (a) interception efficiency model of Spurny (Eq. (18)); (b) interception efficiency model of John (Eq. (20)); and (c) diffusion efficiency model and interception efficiency model of Marre (Eqs. (10-13) and (22-23)) (case of Cyrs et al. (2010)).

Case of R'mili et al. (2013)

R'mili et al. (2013) and Ogura et al. (2014) investigated the sampling efficiencies of mini particle sampler (MPS), with TEM porous grid installed to collect nanoparticles. TEM porous grid consists of a holey carbon film and a copper mesh, as shown in Fig. 10. Here, the case of using "Quantifoil 1.2/1.3" type holey carbon film is analyzed. The structure of this type of carbon film is similar to the Nuclepore filter. According to the work of Ogura et al. (2014), the sampling efficiency due to copper mesh can be ignored. He considered the porosity of the copper mesh and studied the overall sampling efficiency combining the efficiency of carbon film and copper mesh. The theoretical calculation indicated that only a small number of particles were collected on the copper mesh. In addition, very few particles were observed on the copper mesh of the grid during SEM analysis. Particles were mostly captured by holey carbon film since its pore size (1.3 μm) was much smaller than that of the copper mesh (~ 40 μm).

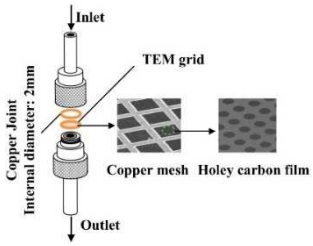

Fig. 10. Structure of MPS (Ogura et al., 2014)

The pore size (measured value) of the used "Quantifoil" carbon film is 1.3 μm and the porosity is 0.17. Even if the thickness of the carbon film is only 0.02 μm, the particle capturing mechanism is the same. NaCl particles within a size range of 15-150 nm were sampled. The tests were performed at a face velocity of 1.6 m/s and a Reynolds number of 0.168. Since the sampling was performed in a circular tube with a small pipe size, the flow type can be considered as laminar flow, or Poiseuille flow. The face velocity was relatively high and the flow viscous was low, thus it would be better to consider flow slip. Eqs. (14), (18), (20), and (27-28) are not eligible in this case.

Considering the flow slip under actual sampling condition, the models of Marre for calculating the diffusion efficiency due to pore wall deposition (Eqs. (10-13)) and interception efficiency (Eqs. (22-23)) are chosen. The model of Manton (Eq. (15)) for calculating the diffusion efficiency due to surface deposition and the model of Pich (Eqs. (24-26)) for calculating the impaction efficiency are suitable since the porosity of used filter is 0.17 and the face velocity is constant. The model of Marre for calculating the combined efficiency of diffusion and interception (Eq. (30)) also can be used. Fig. 11 shows the comparison of experimental and theoretical approaches to assess the overall collection efficiency by Eqs. (1), (29), and (32). Results manifest that both Eqs. (1) and (32) fit the experimental values well. Theoretical efficiency calculated by Eq. (32) is a little higher and closer to the measurements. When particle diameter is in the range of 20-40 nm, all the capturing mechanisms are insignificant, which corresponding to a minimum efficiency, about 15%. Since the filter thickness is 0.02 μm, the ratio of pore length and pore size is small. There are very few particles captured by pore wall. The collection efficiencies due to pore wall deposition (E_{DW}, E_R, and E_{DR}) are less than surface deposition (E_{DS} and E_I) (Smith et al., 1976). However,

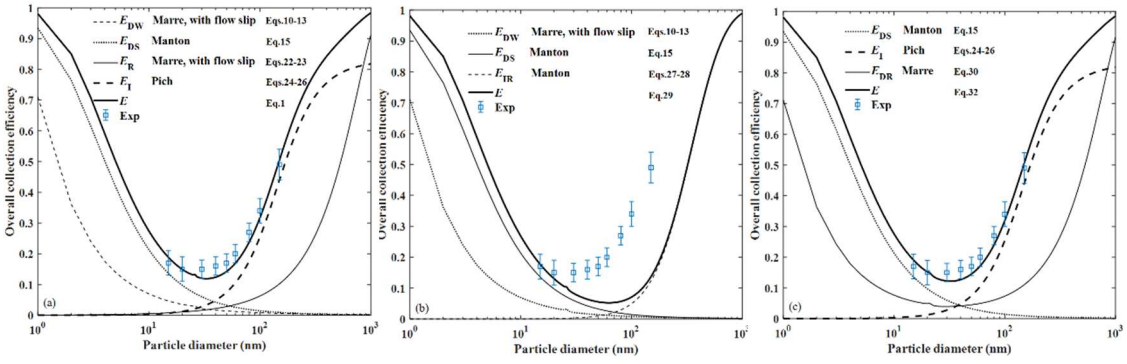

the efficiency simulated with Eq. (29) is much lower than test values because the flow slip can't be ignored in this situation. In addition, the inertia parameter "*I*" in the current test is high (11.16), which is controversial to use the models of Manton (Chen et al., 2013a).

Fig. 11. Comparison of experimental and theoretical approaches for assessing overall collection efficiency using (a) Eq. (1); (b) Eq. (29); and (c) Eq. (32) (case of R'mili et al. (2013)).

5. Conclusion

The review presented here explores the available theoretical models for assessing the sampling efficiency of Nuclepore filters, which involve different particle capturing mechanisms: diffusion, interception, and impaction. Most of the models are based on assumptions. Four models are explored for diffusion efficiency due to pore wall deposition. The model proposed by Marre considered the effect of flow slip, which is important for sampling with high flow velocity. However, this model only fits the intermediate crossover regime between Brownian diffusion and direct interception, which is not appropriate for sampling conditions with big MPPS. For diffusion efficiency due to surface deposition, calculations of Manton are mostly used and verified. For interception deposition, five models are compared for different flow types. Of which, the model proposed by Gentry corresponds to much higher efficiencies for Poiseuille flow, which needs to be prudently used before confirmation. For impaction efficiency, Pich's theory fits laminar flow sampling. In addition, the combined efficiency models have corrected the inappropriateness of considering particle deposition mechanisms separately. If the assumptions are satisfied, they can be recommended.

Experimentally measured values are combined to analyze the effect of the capturing mechanism on collection efficiency. In general, for Nuclepore filters (porosity ≤ 20%, pore size ≤ 12 μm), most of the experimental data are consistent with theoretical efficiencies. All four deposition mechanisms: wall diffusion, surface diffusion, impaction, and interception should be involved in the overall efficiency calculations. For the surface collection efficiency, the contribution of interception deposition should be considered. The overall collection efficiency is higher than the surface collection efficiency, which confirms that particle deposition on the wall of filter pores is essential. In addition, the factors that affect sampling efficiency focusing on filter pore size, face velocity, particle size, and density are reviewed. To capture submicrometer particles effectively, a small pore size with low face velocity or large pore size with high face velocity is recommended, which can maximize the productivity of capturing mechanisms.

When fitting the collection efficiency of filters, the choice of appropriate theoretical models according to the applicable conditions is crucial. A method for combining theoretical model efficiency analysis has been proposed. Models for individual efficiency, combined efficiency, overall efficiency, and surface efficiency are summarized. Two cases are combined to compare the theoretical and experimental efficiencies. The models selected according to the guide fit the experimental values well. More theoretical models need to be simulated for other sampling conditions, such as a surface diffusion model for filters with a porosity of less than 5% and, a flow-slip considered model for calculating combined efficiency of impaction and interception that involves a large range of "*I*" value. This review provides a foundation for more sampling techniques to assess submicrometer particle exposure risks.

Declaration of interests

The authors declare that they have no known competing financial interests or personal relationships that could have appeared to influence the work reported in this paper.

Nomenclatures

A_0 pore area, area occupied by the opening of a radius hole r_0

A_R	total exposed surface area
a, b	*I* - based parameter
Cc	Cunningham correction factor
D	particle diffusion coefficient
$\mathcal{D}$	normalized diffusion coefficient
d_f	filter diameter
E	overall collection efficiency
E_D	collection efficiency due to diffusion
E_{DR}	collection efficiency of diffusion and interception
E_{DS}	collection efficiency due to diffusion on filter surface
E_{DW}	collection efficiency due to diffusion on pore wall
E_I	collection efficiency due to impaction
E_{IR}	combined efficiency of interception and impaction
E_R	collection efficiency due to interception
E_S	surface collection efficiency
I	inertia parameter
K_B	Boltzmann constant
L_f	filter thickness
L_g	slip length
MPPS	most penetrating particle size
ME	minimum efficiency
N_0	number of holes per unit of surface
N_D	diffusion parameter
N_g	slip parameter
N_G	N_g - based parameter
N_r	particle radius normalized for the pore radius
N_R	N_r - based parameter
P	filter porosity
Pe	Peclet's number
Q	flowrate
r_0	filter pore radius
r_c	cylindrical flow radius, external radius of the unit hole
r_p	particle radius
Re	Reynolds number
Stk	Stokes number
T	sampling temperature
U_0	face velocity
y^*	normalized distance
η	fluid dynamic viscosity
ν	fluid kinematic viscosity
ρ	flow density
ρ_p	particle density
γ	*D* - based parameter
Γ	γ - based parameter

α_1 porosity - based parameter

ξ porosity - based parameter

ε_i *Stk* and ξ based parameter

References

Albanese, A., Tang, P.S., Chan, W.C., 2012. The effect of nanoparticle size, shape, and surface chemistry on biological systems. Annual review of biomedical engineering 14, 1-16.

Bressot, C., Shandilya, N., Jayabalan, T., Fayet, G., Voetz, M., Meunier, L., Le Bihan, O., Aguerre-Chariol, O. and Morgeneyer, M., 2018. Exposure assessment of Nanomaterials at production sites by a Short Time Sampling (STS) approach: Strategy and first results of measurement campaigns. Process Safety and Environmental Protection 116, 324-332.

Bulejko, P., 2018. Numerical Comparison of Prediction Models for Aerosol Filtration Efficiency Applied on a Hollow-Fiber Membrane Pore Structure. Nanomaterials 8, 447.

Burton, N.C., Grinshpun, S.A., Reponen, T., 2006. Physical collection efficiency of filter materials for bacteria and viruses. Annals of occupational hygiene 51, 143-151.

Caroff, M., Choudhary, K., Gentry, J., 1973. Effect of pore and particle size distribution on efficiencies of membrane filters. Journal of Aerosol Science 4, 93-102.

Chen, S.-C., Wang, J., Bahk, Y.K., Fissan, H., Pui, D.Y., 2014. Carbon nanotube penetration through fiberglass and electret respirator filter and nuclepore filter media: experiments and models. Aerosol Science and Technology 48, 997-1008.

Chen, S.-C., Wang, J., Fissan, H., Pui, D.Y., 2013a. Use of Nuclepore filters for ambient and workplace nanoparticle exposure assessment—spherical particles. Atmospheric environment 77, 385-393.

Chen, S.-C., Wang, J., Fissan, H., Pui, D.Y., 2013b. Exposure assessment of nanosized engineered agglomerates and aggregates using Nuclepore filter. Journal of nanoparticle research 15, 1955.

Cheng, M.T., Xie, G.W., Fu, T.H. and Shaw, D.T., 1991. Filtration of ultrafine chain aggregate aerosols by Nuclepore filters. Aerosol science and technology 15, 30-35.

Cyrs, W., Boysen, D., Casuccio, G., Lersch, T., Peters, T., 2010. Nanoparticle collection efficiency of capillary pore membrane filters. Journal of Aerosol Science 41, 655-664.

Easty, A., Coakley, N., Cheng, R., Cividino, M., Savage, P., Tozer, R., White, R., 2015. Safe handling of cytotoxics: guideline recommendations. Current Oncology 22, e27.

Elsaesser, A., Howard, C.V., 2012. Toxicology of nanoparticles. Advanced drug delivery reviews 64, 129-137.

Fabiano, B., A.P. Reverberi., P.S. Varbanov., 2019. Safety opportunities for the synthesis of metal nanoparticles and short-cut approach to workplace risk evaluation. Journal of Cleaner Production 209, 297-308.

Fan, K.-C., Gentry, J.W., 1978a. Clogging in nuclepore filters. Environmental Science & Technology 12, 1289-1294.

Fan, K., Leaseburge, C., Hyun, Y., Gentry, J., 1978b. Clogging in Nuclepore filters: cap formation model. Atmospheric Environment 12, 1797-1802.

Fleischer, R.L., Price, P.B., Walker, R.M., 1965. Tracks of charged particles in solids. Science 149, 383-393.

Fuchs, N.A., Daisley, R., Fuch, M., Davies, C., Straumanis, M.,1965. The mechanics of aerosols. Physics Today 18, 73.

Gao, H., He, W., Yu, R., Hammer, T., Xu, G. and Wang, J., 2020. Aerodynamic property and filtration evaluation of airborne graphene nanoplatelets with plate-like shape and folded structure. Separation and Purification Technology, 117293.

Gentry, J., Spurny, K., Schoermann, J., 1982. Diffusional deposition of ultrafine aerosols on nuclepore filters. Atmospheric Environment 16, 25-40.

Gentry, J.W. and Spurny, K.R., 1978. Measurements of collection efficiency of nuclepore filters for asbestos fibers. Journal of Colloid and Interface Science 65, 174-180.

Godoi, R.H., Gonçalves, S.J., Sayama, C., Polezer, G., Neto, J.M.R., Alföldy, B., Van Grieken, R., Riedi, C.A., Yamamoto, C.I., Godoi, A.F., 2016. Health implications of atmospheric aerosols from asbestos-bearing road pavements traditionally used in Southern Brazil. Environmental Science and Pollution Research 23, 25180-25190.

Gormley, P., Kennedy, M., 1948. Diffusion from a stream flowing through a cylindrical tube, Proceedings of the Royal Irish Academy. Section A: Mathematical and Physical Sciences. JSTOR, pp. 163-169.

Hampl, V., Spurný, K., 1966. Analytical methods for determination of aerosols by means of membrane ultrafilters. VIII. Determination of

the mean pore size by gas flow rate measurements. Collection of Czechoslovak Chemical Communications 31, 1152-1161.

Happel, J., Brenner, H., 2012. Low Reynolds number hydrodynamics: with special applications to particulate media. Springer Science & Business Media.

Heidam, N.Z., 1981. Aerosol fractionation by sequential filtration with Nuclepore filters. Atmospheric Environment 15, 891-904.

Hinds, W.C., 1999. Aerosol technology: properties, behavior, and measurement of airborne particles. John Wiley & Sons.

Hinds, W.C., 2012. Aerosol technology: properties, behavior, and measurement of airborne particles. John Wiley & Sons.

Huang, H.-L., Yang, S., 2006. Filtration characteristics of polysulfone membrane filters. Journal of aerosol science 37, 1198-1208.

Jeffery, G.B., 1922. The motion of ellipsoidal particles immersed in a viscous fluid. Proceedings of the Royal Society of London. Series A, Containing papers of a mathematical and physical character 102, 161-179.

John, W., Reischl, G., 1978. Measurements of the filtration efficiencies of selected filter types. Atmospheric Environment 12, 2015-2019.

Lafleur, J.E., Rice, S.A., 2015. Induction of resistance to S. aureus in an environmental marine biofilm grown in Sydney Harbor, NSW, Australia. World Journal of Microbiology and Biotechnology 31, 353-358.

Li, M.-Z., Cai, Z.-Y., Sui, Z., Yan, Q., 2002. Multi-point forming technology for sheet metal. Journal of Materials Processing Technology 129, 333-338.

Liu, B.Y., Lee, K., 1976. Efficiency of membrane and nuclepore filters for submicrometer aerosols. Environmental Science & Technology 10, 345-350.

Liu, B.Y., Pui, D.Y., Rubow, K., 1983. Characteristics of air sampling filter media, Unknown Host Publication Title.

Manton, M., 1978. The impaction of aerosols on a nuclepore filter. Atmospheric Environment 12, 1669-1675.

Manton, M., 1979. Brownian diffusion of aerosols to the face of a nuclepore filter. Atmospheric Environment 13, 525-531.

Marre, S., Palmeri, J., 2001. Theoretical study of aerosol filtration by nucleopore filters: the intermediate crossover regime of Brownian diffusion and direct interception. Journal of colloid and interface science 237, 230-238.

Marre, S., Palmeri, J., Larbot, A., Bertrand, M., 2004. Modeling of submicrometer aerosol penetration through sintered granular membrane filters. Journal of colloid and interface science 274, 167-182.

Mathis, U., Kaegi, R., Mohr, M., Zenobi, R., 2004. TEM analysis of volatile nanoparticles from particle trap equipped diesel and direct-injection spark-ignition vehicles. Atmospheric Environment 38, 4347-4355.

Mengersen, K., Morawska, L., Wang, H., Murphy, N., Tayphasavanh, F., Darasavong, K., Holmes, N., 2011. Association between indoor air pollution measurements and respiratory health in women and children in Lao PDR. Indoor air 21, 25-35.

Mercer, T., Greene, T., 1974. Interpretation of diffusion battery data. Journal of Aerosol Science 5, 251-255.

Methner, M., Beaucham, C., Crawford, C., Hodson, L., Geraci, C., 2012. Field application of the Nanoparticle Emission Assessment Technique (NEAT): task-based air monitoring during the processing of engineered nanomaterials (ENM) at four facilities. Journal of occupational and environmental hygiene 9, 543-555.

Methner, M., Hodson, L., Dames, A., Geraci, C., 2010. Nanoparticle emission assessment technique (NEAT) for the identification and measurement of potential inhalation exposure to engineered nanomaterials—Part B: Results from 12 field studies. Journal of occupational and environmental hygiene 7, 163-176.

Montassier, N., Dupin, L., Boulaud, D., 1996. Experimental study on the collection efficiency of membrane filters. Journal of Aerosol Science 27, S637-S638.

Morgeneyer, M., Aguerre-Chariol, O., Bressot, C., 2018. STEM imaging to characterize nanoparticle emissions and help to design nanosafer paints. Chemical Engineering Research and Design 136, 663-674.

Natanson, G., 1957. Diffusive deposition of aerosols on a cylinder in a flow in the case of small capture coefficients, Doklady Akademii Nauk. Russian Academy of Sciences, pp. 100-103.

Ogura, I., Hashimoto, N., Kotake, M., Sakurai, H., Kishimoto, A., Honda, K., 2014. Aerosol particle collection efficiency of holey carbon film-coated TEM grids. Aerosol Science and Technology 48, 758-767.

Ogura, I., Kotake, M., Sakurai, H., Honda, K., 2016. Surface-collection efficiency of Nuclepore filters for nanoparticles. Aerosol Science and Technology 50, 846-856.

Park, Y., King Jr, W., Gentry, J., 1980. On the inversion of penetration measurements to determine aerosol product size distributions. Industrial & Engineering Chemistry Product Research and Development 19, 151-157.

Pich, J., 1964. Impaction of aerosol particles in the neighbourhood of a circular hole. Collection of Czechoslovak Chemical Communications 29, 2223-2227.

Price, P., Walker, R., 1962. Chemical etching of charged-particle tracks in solids. Journal of applied physics 33, 3407-3412.

R'mili, B., Le Bihan, O.L., Dutouquet, C., Aguerre-Charriol, O., Frejafon, E., 2013. Particle sampling by TEM grid filtration. Aerosol Science and Technology 47, 767-775.

Romo-Kröger, C.M., 2006. A qualitative study of atmospheric aerosols and particles deposited on flat membrane surfaces by microscopy and other techniques. Powder technology 161, 235-241.

Rubow, K., Liu, B., 1986. Characteristics of membrane filters for particle collection, Fluid Filtration: Gas Volume I. Astm International.

Rubow, K.L., 1981. Submicron Aerosol Filtration Characteristics of Membrane Filters. University of Minnesota.

Salma, I., Füri, P., Németh, Z., Balásházy, I., Hofmann, W., Farkas, Á., 2015. Lung burden and deposition distribution of inhaled atmospheric urban ultrafine particles as the first step in their health risk assessment. Atmospheric Environment 104, 39-49.

Schmid, O., Stoeger, T., 2016. Surface area is the biologically most effective dose metric for acute nanoparticle toxicity in the lung. Journal of Aerosol Science 99, 133-143.

Shatkin, J.A., 2017. Nanotechnology: health and environmental risks. Crc Press.

Slezakova, K., Morais, S., do Carmo Pereira, M., 2013. Atmospheric nanoparticles and their impacts on public health, Current topics in public health. IntechOpen.

Smith, T.N., Phillips, C.R., Melo, O.T., 1976. Diffusive collection of aerosol particles on Nuclepore membrane filter. Environmental Science & Technology 10, 274-277.

Soo, J.-C., Monaghan, K., Lee, T., Kashon, M., Harper, M., 2016. Air sampling filtration media: Collection efficiency for respirable size-selective sampling. Aerosol Science and Technology 50, 76-87.

Spurny, K., Lodge, J.P., Frank, E.R., Sheesley, D.C., 1969. Aerosol filtration by means of Nuclepore filters: structural and filtration properties. Environmental Science & Technology 3, 453-464.

Spurný, K., Pich, J., 1963. Analytical methods for determination of aerosols with help of membrane ultrafilters. VI. On the mechanism of membrane ultrafilter action. Collection of Czechoslovak Chemical Communications 28, 2886-2894.

Spurny, K., Pich, J., 1964. Zur frage der Filtrationmechanismen bei Membranfiltern. Staub 24, 250.

Spurny, K., Pich, J., 1965. Analytical methods for determination of aerosols by means of membrane ultrafilters. VII. Diffusion and impaction precipitation of aerosol particles by membrane ultra-filters. Collection of Czechoslovak Chemical Communications 30, 2276-2287.

Spurny, K. R., 1998. Pore filters: aerosol filtration and sampling. Advances in aerosol filtration.

Todea, A.M., Beckmann, S., Kaminski, H., Bard, D., Bau, S., Clavaguera, S., Dahmann, D., Dozol, H., Dziurowitz, N., Elihn, K., Fierz, M., 2017. Inter-comparison of personal monitors for nanoparticles exposure at workplaces and in the environment. Science of the Total Environment 605, 929-945.

Twomey, S., 1962. Equations for the decay of diffusion of particles in an aerosol flowing through circular or rectangular channels. Bull Observ Puy de Dome 10, 173-180.

Yamamoto, N., Fujii, M., Kumagai, K., Yanagisawa, Y., 2004. Time course shift in particle penetration characteristics through capillary pore membrane filters. Journal of aerosol science 35, 731-741.

Zíková, N., Ondráček, J., Ždímal, V., 2015. Size-Resolved Penetration Through High-Efficiency Filter Media Typically Used for Aerosol Sampling. Aerosol Science and Technology 49, 239-249.

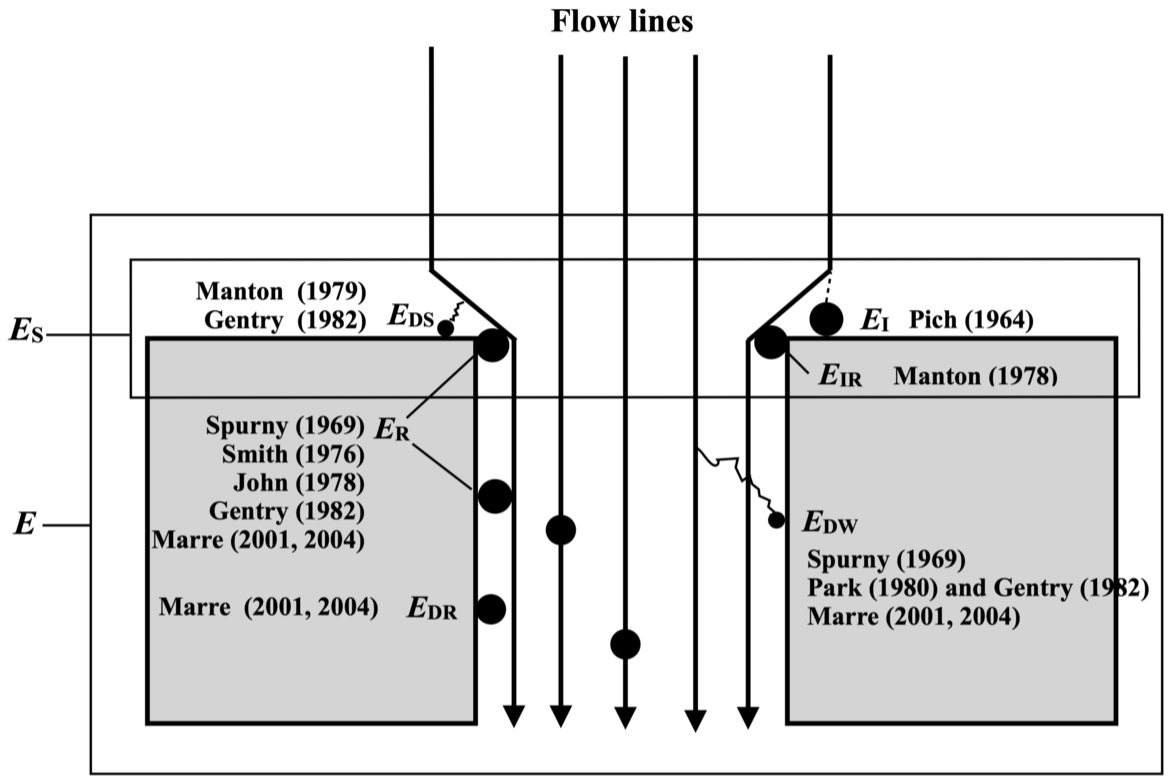

$E_S=1-(1-E_{DS})(1-E_I)$ **Cyrs (2010)**	$E=1-(1-E_{DW})(1-E_{DS})(1-E_R)(1-E_I)$ **Hinds (1999)**
$E_S=1-(1-E_{DS})(1-E_R)(1-E_I)$ **Chen (2013a)**	$E=1-(1-E_{IR})(1-E_{DW})(1-E_{DS})$ **Manton (1978)**
$E_S=1-(1-E_{DS})(1-E_{IR})$ **Ogura (2016)**	(**correct** the inadequateness of considering E_I and E_R separately)
	$E=1-(1-E_{DR})(1-E_{DS})(1-E_I)$ **Marre (2001, 2004)**
	(**correct** the inadequateness of considering E_{DW} and E_R separately)